Leadzyme formed *in vivo* interferes with tobacco mosaic virus infection in *Nicotiana tabacum*

Eliza Wyszko[1], Monika Nowak[1], Henryk Pospieszny[2], Maciej Szymanski[1], Jakub Pas[1,3], Mirosława Z. Barciszewska[1] and Jan Barciszewski[1]

1 Institute of Bioorganic Chemistry, Polish Academy of Sciences, Poznan, Poland
2 Institute of Plant Protection, Department of Virology and Bacteriology, Poznan, Poland
3 BioInfoBank Institute, Poznan, Poland

We developed a new method for inhibiting tobacco mosaic virus infection in tobacco plants based on specific RNA hydrolysis induced by a leadzyme. We identified a leadzyme substrate target sequence in genomic tobacco mosaic virus RNA and designed a 16-mer oligoribonucleotide capable of forming a specific leadzyme motif with a five-nucleotide catalytic loop. The synthetic 16-mer RNA was applied with nontoxic, catalytic amount of lead to infected tobacco leaves. We observed inhibition of tobacco mosaic virus infection in tobacco leaves *in vivo* due to specific tobacco mosaic virus RNA cleavage effected by leadzyme. A significant reduction in tobacco mosaic virus accumulation was observed even when the leadzyme was applied up to 2 h after inoculation of leaves with tobacco mosaic virus. This process, called leadzyme interference, is determined by specific recognition and cleavage of the target site by the RNA catalytic strand in the presence of Pb^{2+}.

Catalytic RNAs (ribozymes) are capable of specific binding and cleaving of RNA molecules. Since their discovery, many efforts have been made to explore them as tools for silencing of viral genes and inhibition of viral growth [1]. Generally, there are two modes of application and delivery of catalytic RNAs to the cell. The first is a gene therapy approach, in which a gene encoding the ribozyme is cloned into a vector [2]. After transfection or transduction, the gene becomes stably integrated in the host DNA, and its transcription provides a continuous intracellular supply of the ribozyme. This approach has been used to deliver various types of catalytic RNAs, such as hammerhead, hairpin or M1 RNA of RNase P [2,3]. In the second method, synthetic ribozymes are added to cells from the outside. Efficient cleavage of the cellular target requires the presence of divalent metal ions, in particular Mg^{2+}, which is virtually the only divalent metal ion available at millimolar con-

centrations under normal intracellular conditions [4]. As RNA is chemically unstable and undergoes spontaneous degradation at neutral pH [5] the ribozyme elements that are not crucial for catalytic activity (e.g. recognition sequences) are often modified to increase stability [6–8].

One of the RNA-cleaving agents is a leadzyme that has been identified as a small RNA motif consisting of a six-nucleotide asymmetric purine-rich loop within the RNA duplex. Such a motif is capable of autocatalytic cleavage in the presence of Pb^{2+} [9,10]. Because of its small size and high specificity, the leadzyme has been studied extensively. NMR and X-ray crystallography [11–14] as well as kinetic studies [15] have been carried out to elucidate its structure, conformational dynamics and hydrolytic properties. The most important question is how this small RNA binds to and deploys a divalent cation (Pb^{2+}) to catalyze the cleavage reaction in a similar way to other ribozymes and RNase A [9].

Like other ribozymes, the leadzyme has been used for sequence-specific hydrolysis of a variety of RNA molecules. Recently, we used this approach for structural studies on 5S ribosomal RNA [16]. In that study, a mammalian 5S rRNA's loop D was shown to bind a synthetic complementary oligonucleotide to form a leadzyme motif which, in the presence of Pb^{2+}, cleaves an RNA substrate strand. These experiments confirmed the presence of a nine-nucleotide D loop in mammalian 5S rRNA, and demonstrated the usefulness of leadzymes as tools in structural studies of nucleic acids [16].

The inhibition of gene expression by RNA is currently recognized as one of the major gene regulation mechanisms in biology. RNA silencing mediates defensive responses against viruses [20], but on the other hand, it can be used as a tool directed against molecular parasites. To achieve this goal, we analyzed the inhibition of tobacco mosaic virus (TMV) as a model system for inhibiting viral infections caused by positive single-stranded RNA (+)ssRNA viruses.

Currently, we are facing various threats of epidemic diseases. Many of them are caused by viruses with genomes composed of (+)ssRNA. Many of the human and animal viruses belong to this group. It includes, for example, rubellavirus, poliovirus, rhinoviruses, yellow fever virus, West Nile virus, hepatitis A virus, hepatitis C virus and large family of coronaviruses, including severe acute respiratory syndrome coronavirus [17–19].

In this article, we show that exogenous ssRNA with sequence complementarity binds the target site in TMV RNA to form a leadzyme motif, and in the presence of a catalytic amount of Pb^{2+}, cleaves viral (+)ssRNA. As a consequence, viral infection in *Nicotiana tabacum* leaves is suppressed. This approach demonstrated that the catalytic leadzyme strand can be introduced into the cell, where it performs its hydrolytic function, which interferes with virus or protein synthesis.

Results

The anti-TMV leadzyme

A leadzyme with a five-nucleotide internal loop was selected as a model for design of an anti-TMV leadzyme (Fig. 1A). The target sequences in TMV RNA were found in a complete TMV genome using the well-known leadzyme motif. To design an active leadzyme, we analyzed the sequences of all available TMV strains. Two putative target palindromic CGAGC motifs were found in the genomic strand of TMV
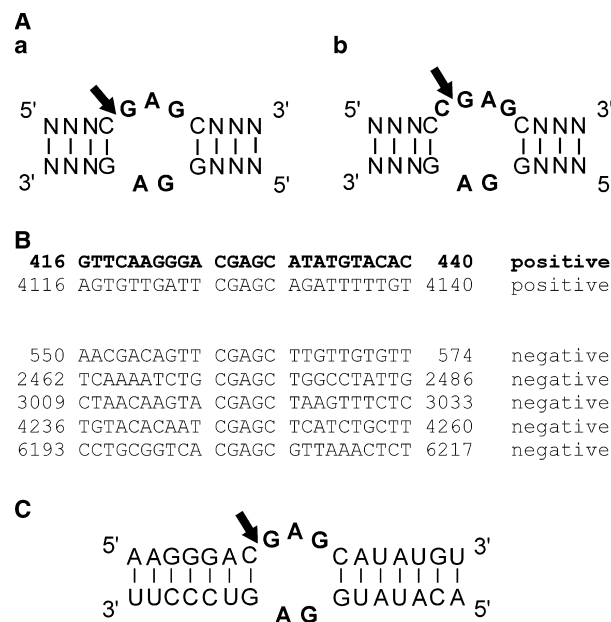

Fig. 1. The structure of a leadzyme. (A) Secondary structures of six-nucleotide (a) and five-nucleotide (b) active centre leadzymes. The asymmetric, purine-rich internal loop (five or six nucleotides) forms the catalytic core of the leadzyme. Cleavage occurs on the substrate strand only in the presence of Pb^{2+}. N, any nucleotide. (B) Putative targets for leadzyme formation selected in genomic strand (+)ssRNA (marked as positive) and antigenomic strand (–)ssRNA (marked as negative) of TMV. Numbers show nucleotides in the TMV RNA molecule. The RNA sequence chosen for the anti-TMV leadzyme is in bold. (C) The secondary structure of the anti-TMV leadzyme used in this study. It was constructed on the basis of our previous experiments with 5S rRNA [16]. Upper strand, target (a fragment of the TMV sequence); lower strand, catalytic strand. The scissile bond is marked by an arrow.

(+)ssRNA, and four in the antigenomic (–)ssRNA) strand (Fig. 1A). The structure of the leadzyme target sites was analyzed using RNA-prediction program MFOLD to select only those TMV RNA sequences for which a single-strand structure was more likely in a probabilistic model [25]. The sequence (416) 5′-GUUCAAGGGACGAGCAUAUGUACAC-3′ (440) was predicted not to be involved in the formation of a stable secondary structure and was used in further studies (Fig. 1B). This sequence is present in all TMV strains. The localization of this motif close to the 5′-end of the TMV genome within the replicase-coding sequence (ORF 1) was an additional advantage. The designed catalytic strand of the leadzyme was a 16-nucleotide RNA (5′-ACAUAUGGAGUCCCUU-3′), and its binding to the target sequence results in the formation of the leadzyme motif with a five-nucleotide internal loop (Fig. 1C). The activity of the anti-TMV leadzyme
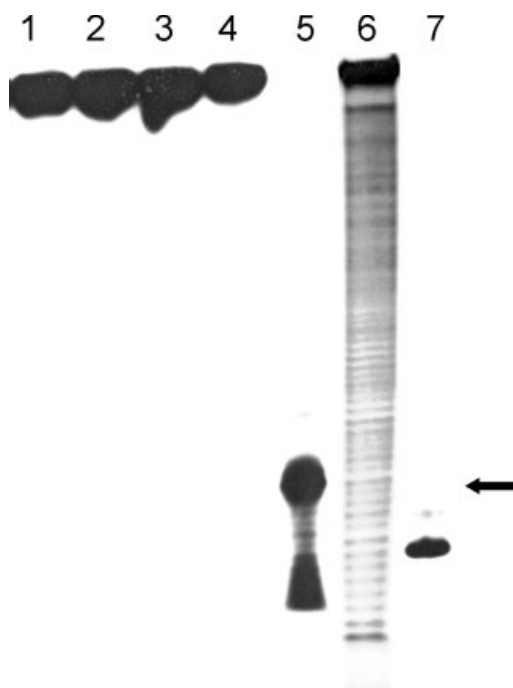
Fig. 2. *In vitro* cleavage of the TMV RNA fragment (100-mer oligo). The autoradiogram of 10% PAGE containing 7 M urea shows hydrolysis products of the 100-nucleotide TMV RNA fragment labeled at the 5′-end by the anti-TMV leadzyme. The reaction was carried out at 25 °C for 1 h. Lanes: 1, substrate TMV RNA in water; 2, substrate TMV RNA in 15 mM Mops (pH 7.5); 3, substrate RNA in Mops and Pb^{2+} (250 μM); 4, substrate RNA in Mops and leadzyme (25 μM); 5, substrate RNA in Mops, leadzyme (25 μM) and Pb^{2+} (250 μM); 6, ladder, alkaline hydrolysis; 7, molecular size marker (29 nucleotides). The arrow indicates the site of RNA TMV hydrolysis by the leadzyme (37 nucleotides).

was confirmed *in vitro* by cleavage of 100-nucleotide TMV RNA using the catalytic strand of the leadzyme and Pb^{2+} (Fig. 2). The cleavage site occurred before the first residue (between C and G) of an internal loop on a target strand and only in the presence of Pb^{2+}.

Specific inhibition of TMV infection in plant cells by the leadzyme

Using the designed anti-TMV leadzyme, we investigated whether the leadzyme motif can be formed and perform its hydrolytic functions *in vivo*. The catalytic RNA strand of the leadzyme and Pb^{2+} were directly delivered (mechanical inoculation) together with TMV to *Nicotiana tabacum* cv. Xanti-nc, a hypersensitive local lesion host. To evaluate the optimal Pb^{2+}/RNA ratio for efficient TMV inhibition, *Nicotiana tabacum* leaves were inoculated with mixtures composed of TMV, catalytic RNA and Pb^{2+} prepared just before

inoculation. TMV genomic RNA is enclosed within the protein capsid, and as a result, leadzyme formation and TMV RNA cleavage is possible only within host cells. RNA was applied at four concentrations of 2.5, 5, 12 and 25 μM combined with 0.5, 1, 5 and 10 μM Pb^{2+}. At 4–5 days postinoculation, the amount of symptoms of infection manifested as local lesions was compared to that in control plants, i.e. inoculated with TMV alone or with TMV in the presence of RNA or Pb^{2+} at the same concentrations as indicated above. Control assays, with 16-nucleotide catalytic RNA only or Pb^{2+} applied in the presence of TMV, were performed to demonstrate the specificity of leadzyme cleavage. For each single assay, at least three plants were inoculated with the same mixtures, for both control and experimental assays. The number of local lesions was the basis for rejecting RNA and Pb^{2+} concentrations at which disease symptoms were observed to a similar extent as in controls. In further experiments, 2.5 μM catalytic RNA with 1, 5 and 10 μM Pb^{2+} were tested. This corresponds to 0.4, 2 and 4 Pb^{2+}/RNA, respectively (Fig. 3A,B). Coinoculation of TMV and 2.5 μM RNA with 1, 5 and 10 μM Pb^{2+} led to a decreased number of a local lesions (~ 15) in comparison with control plants (~ 80) (Fig. 3A,B). The results of quantitative local lesion assays were confirmed by RT-PCR analysis. They showed a lower level of TMV after treatment with a two-fold excess of Pb^{2+} over catalytic RNA (Fig. 3C, lane 3), whereas in control leaves infected with virus alone, TMV was detectable (Fig. 3C, lanes 1 and 2).

Time effect on specific TMV inhibition with the leadzyme

The inhibitory effect on TMV was observed up to 8 days of plant incubation. The number of local lesions was the same up to 5 days. To verify the ability of the leadzyme to efficiently inhibit virus during lasting infection, both RNA and Pb^{2+} were applied together with TMV at time 0 or 2 and 4 h later after the infection of *Nicotiana tabacum* cv. Xanti-nc. In these experiments, 2.5 μM RNA and 5 μM Pb^{2+} were used (Fig. 4A,B). Control assays were performed with 2.5 μM RNA and 5 μM Pb^{2+} applied separately with TMV (Fig. 4A, columns 3 and 4). We also tested control plants that were uninfected and treated only with TMV (Fig. 4A, columns 1 and 2). Reduced necrosis due to RNA and Pb^{2+} application was observed in three independent experiments (Fig. 4A,B). The lowest TMV level was observed when RNA, Pb^{2+} and TMV were inoculated simultaneously (~ 15 local lesions), although delayed leadzyme application also resulted in
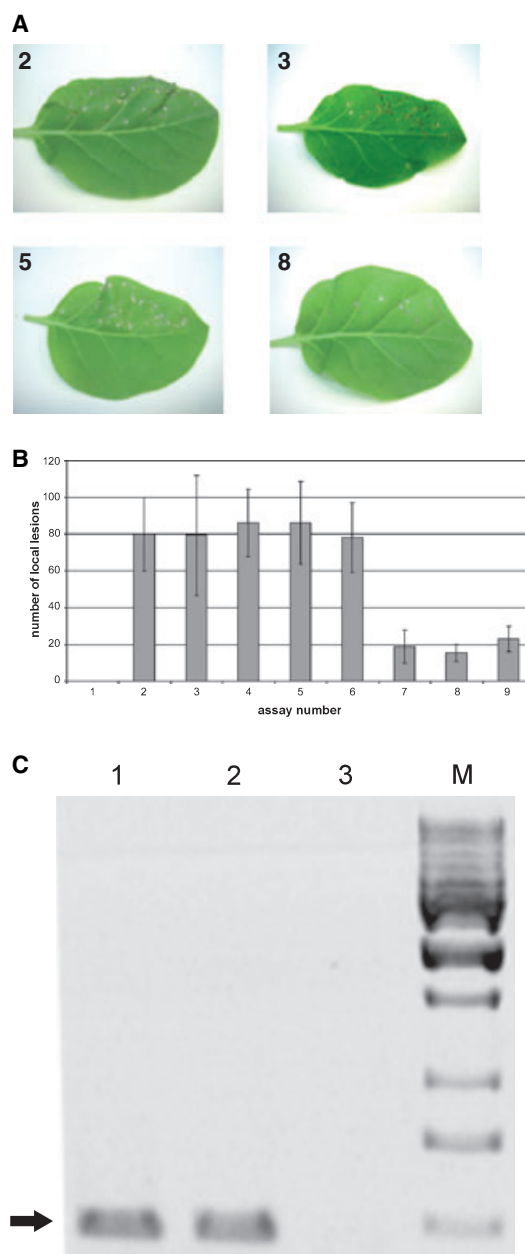
Fig. 3. Inhibition of TMV infection by the leadzyme in *Nicotiana tabacum* cv. Xanti-nc leaves. (A) Tobacco leaves with symptoms of TMV infection. Numbers indicate tobacco leaves inoculated, as in (B). Only the upper half of each leaf was inoculated. The lower halves were used as negative controls. Leaves were photographed at 5 days postinoculation. (B) Number of local lesions observed on tobacco leaves in response to TMV: 2, 5 $\mu g \cdot mL^{-1}$; 3, TMV (5 $\mu g \cdot mL^{-1}$) and 2.5 μM catalytic RNA; 4, TMV (5 $\mu g \cdot mL^{-1}$) and 1 μM Pb^2; 5, TMV (5 $\mu g \cdot mL^{-1}$) and 5 μM Pb^2; 6, TMV (5 $\mu g \cdot mL^{-1}$) and 10 μM Pb^2; 7, TMV (5 $\mu g \cdot mL^{-1}$), 2.5 μM catalytic RNA and 1 μM Pb^{2+} 8, TMV (5 $\mu g \cdot mL^{-1}$), 2.5 μM catalytic RNA and 5 μM Pb^2; 9, TMV (5 $\mu g \cdot mL^{-1}$), 2.5 μM catalytic RNA and 10 μM Pb^2; 1, an uninfected control plant. Representative data (± SEM) from at least three independent experiments are shown. (C) Electrophoretic analysis on 1.5% agarose gel of RT-PCR products of TMV inhibition with leadzyme. Total RNA was extracted from infected leaves of *Nicotiana tabacum* cv. Xanti-nc that had been inoculated with: TMV (5 $\mu g \cdot mL^{-1}$) – lane 1; TMV and 5 μM Pb^{2+} – lane 2; TMV, 2.5 μM leadzyme and 5 μM Pb^{2+} – lane 3. RT-PCR products were stained with ethidium bromide. An arrow indicates PCR products (470 bp). M, 100 bp molecular size marker.

a significant decrease in infection (on average, 25 local lesions). In control plants, the number of local lesions was comparable, ranging from 80 to 110. RT-PCR analysis of total RNA extracted from inoculated leaves confirmed those observations. Decreased TMV RNA expression was observed in leaves treated with RNA and Pb^{2+}, whereas virus expression in control plants was at a high level (Fig. 5A). A reference RT-PCR with β-actin primers was performed (Fig. 5A). The strongest TMV inhibition by the leadzyme occurred in coinoculation assays, although there was still a strong effect after 2 h and and a weaker effect after 4 h delayed leadzyme application.

The amount of cDNA of TMV amplified with RT-PCR was estimated by phosphoimager analysis (Fig. 5B). It was normalized to the control leaves infected with TMV alone (100%). This analysis showed comparable levels of TMV in controls with RNA applied both with TMV (89%) as well as in controls with Pb^{2+} and TMV (92%). The samples amplified with a template obtained from leaves treated with catalytic RNA and Pb^{2+} demonstrated reduced amounts of cDNA TMV: 26%, 51% and 64% when RNA and Pb^{2+} were added simultaneously with TMV, or 2 and 4 h after inoculation with TMV, respectively.

Discussion

Ribozymes can be designed to cleave substrate RNAs in a sequence-specific manner and are important tools for specific inhibition of the expression of deleterious genes [27–29]. The therapeutic development of catalytic RNAs has faced many problems concerning stability, activity and delivery of RNA into the cells *in vivo* [1,28,30]. In the last few years, much attention has been paid to RNA interference (RNAi), a dsRNA-guided post-transcriptional gene-regulatory silencing mechanism that exists in virtually all eukaryotes. This evolutionarily conserved process is involved in defense against transposones and viruses [31–33]. However, there are some problems with inhibition of viral infections with RNAi. To escape RNAi-mediated
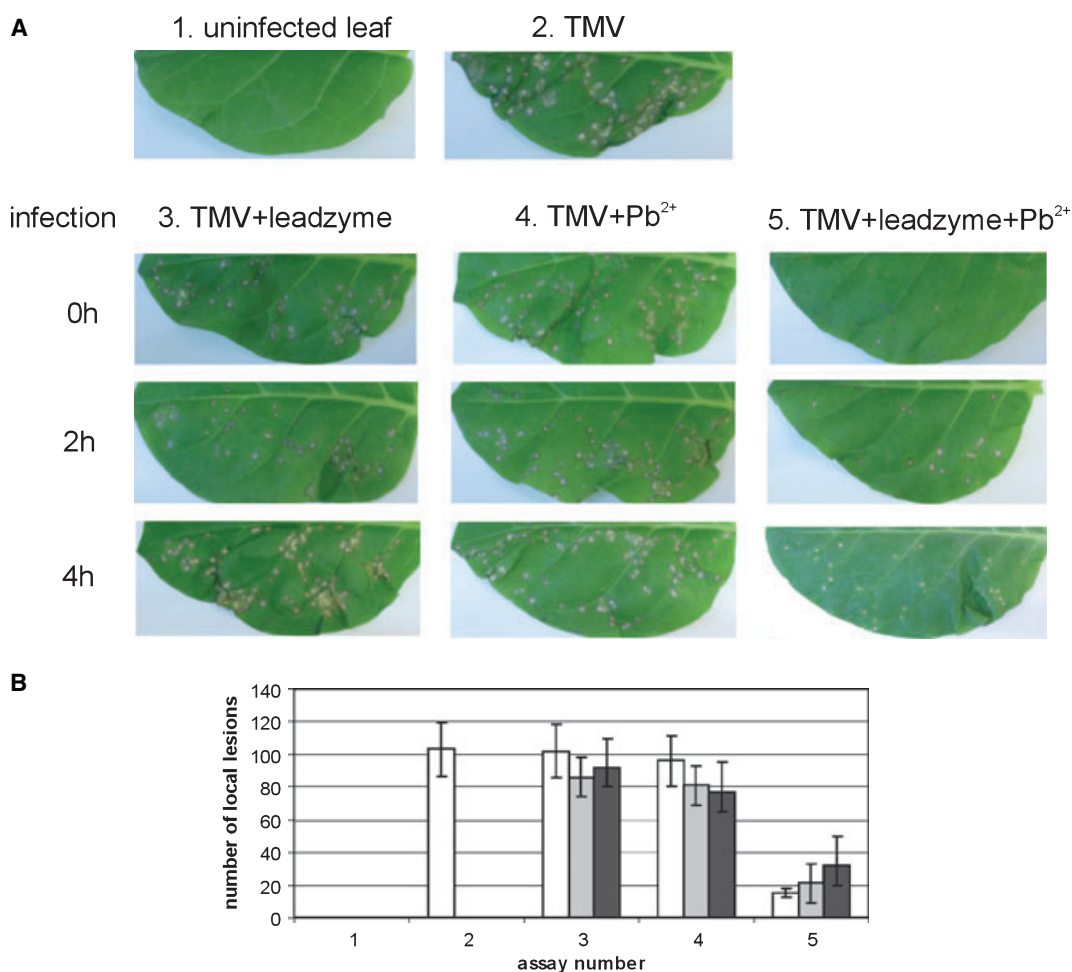
A

1. uninfected leaf

2. TMV

infection

3. TMV+leadzyme

4. TMV+Pb^{2+}

5. TMV+leadzyme+Pb^{2+}

0h

2h

4h

B

Fig. 4. Time-dependent TMV inhibition by the leadzyme in *Nicotiana tabacum* cv. Xanti-nc plants. (A) The response of tobacco leaves to coinoculation with TMV, RNA (leadzyme catalytic strand) and/or Pb^{2+} or delayed inoculation with RNA/Pb^{2+} after previous TMV infection. RNA and/or Pb^{2+} were applied together with TMV (0 h) or 2 h and 4 h after TMV infection. (B) The level of local lesions on infected tobacco leaves inoculated with leadzyme and/or Pb^{2+} in a time-dependent way. Numbers indicate the experimental assays: 1, an uninfected plant; 2, plant inoculated with TMV alone; 3, TMV and catalytic RNA (2.5 µM); 4, TMV and Pb^{2+} (5 µM); 5, TMV, catalytic RNA and Pb^{2+}. White columns, coinoculation with TMV/catalytic RNA/Pb^{2+} (0 h); gray and black columns, separate dosing with a catalytic RNA/Pb^{2+} mixture at, respectively, 2 and 4 h after TMV infection (2 h, 4 h). Representative data (± SEM) from at least three independent experiments are shown.

inhibition, viruses evolved a defense strategy to overcome RNA silencing [34]. Many RNAi suppressors have been identified in plant, animal and insect viruses [34]. The best characterized are potyvirus-encoded helper component proteinase HcPro [49,50], cytomegalovirus-encoded 2b protein [49] and p25 protein identified in potato virus X [51]. An RNAi suppressor has also been found among members of the *Tobamovirus* genus (including TMV and tomato mosaic virus) [34,52]. Suppressors are commonly involved in the enhancement of viral pathogenicity and accumulation of the viruses. It has been shown that these factors act at different steps in the RNAi pathway, e.g. prevention of siRNA production, siRNA binding or spread

of the silencing signal [34,52]. Another important but undesirable aspect of the RNAi process is induction of nonspecific effects by siRNAs. At the mRNA level, this is connected with an 'off-target effect' – nonspecific degradation of transcripts. At the protein level, dsRNA delivery can activate RNA-dependent protein kinase (PKR), 2'5'-oligoadenylate synthetase, the interferon response that leads to the cell death [35,36]. To avoid these negative RNAi effects, we developed a new, efficient approach. It is based on the formation of the leadzyme motif in *trans* and hydrolysis of target RNA.

To examine the ability of the leadzyme to function *in vivo*, the synthetic RNA was introduced into the
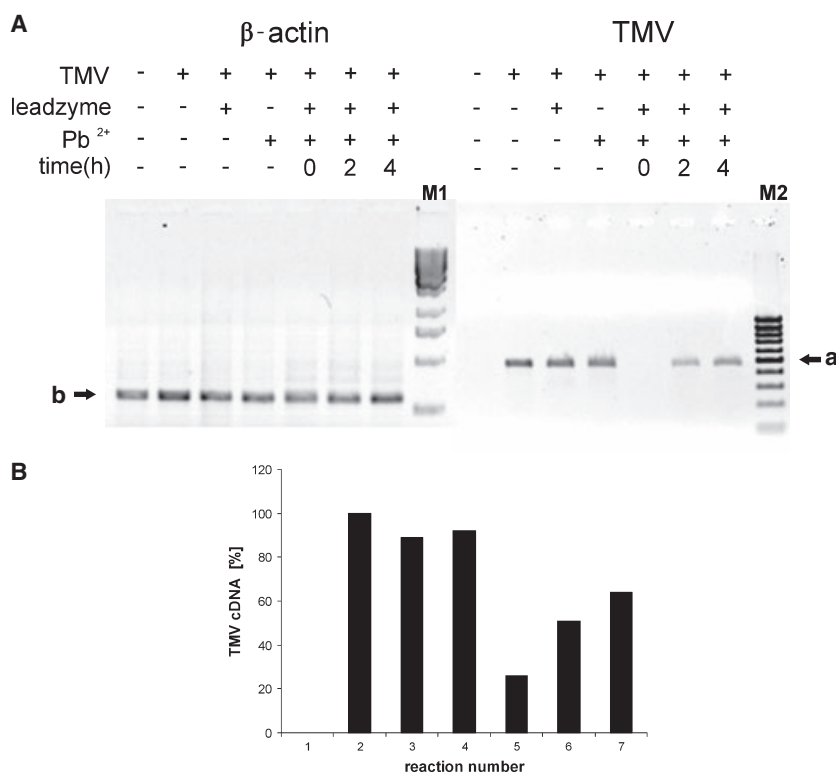
Fig. 5. Effect of leadzyme on TMV expression in a time-dependent RT-PCR experiment. (A) RT-PCR analysis of TMV expression on a 1.5% agarose gel stained with ethidium bromide. The level of TMV infection in plants inoculated with TMV, catalytic RNA and Pb^{2+}, respectively, as shown in the table, was analyzed using RNA templates isolated from tobacco leaves and primers binding upstream and downstream of the scissile bond on a target strand. RT-PCR experiments were performed to compare the levels of TMV in control plants and infected tobacco plants treated with catalytic RNA (2.5 μM) and Pb^{2+} (5 μM). Catalytic RNA and/or Pb^{2+} were applied together with TMV (0 h) or 2 h and 4 h after TMV infection. A reference RT-PCR was performed using the same RNA templates and β-actin primers. Arrows indicate RT-PCR products: (a), 470 bp (TMV band); (b), 300 bp (β-actin band); M1, 1 kb molecular size marker ladder; M2, 100 bp molecular size marker ladder. (B) Evaluation of the amount of cDNA TMV using phosphoimager analysis (IMAGEQUANT). Reaction numbers indicate RT-PCR products amplified with TMV primers as shown in (A): 1, uninfected tobacco; 2, TMV;, 3, TMV and catalytic RNA; 4, TMV and Pb^{2+} 5, TMV, catalytic RNA and Pb^{2+} inoculated simultaneously (0 h); 6, catalytic RNA and Pb_{2+} dosed 2 h postinfection; 7, catalytic RNA and Pb^{2+} dosed 4 h post-infection. Calculations were normalized to control assay with TMV alone (100%).

Nicotiana tabacum cv. Xanti-nc host plants together with Pb^{2+} and TMV. This model system has several advantages. TMV is a highly infectious (+)ssRNA virus. The symptoms of infection can be easily evaluated (local lesions are countable) and observed in a short time period (4–5 days). In the TMV genome, we identified the specific cleavage target for a leadzyme. Two conserved CGAGC sequences were found in TMV genomes. The target sequence near the 5′-end located within ORF 1 encoding viral replicase was further analyzed. We designed and synthesized a catalytic 16-nucleotide RNA strand capable of forming a leadzyme with TMV RNA. It consists of a five-nucleotide asymmetric loop surrounded by two dsRNA regions (Fig. 1C). The leadzyme with the internal loop composed of five nucleotides shows a higher rate of hydrolysis ($k_{obs} = 1.4 \times 10^{-1}$ min^{-1}) when compared to

the 'classic' leadzyme with a six-nucleotide internal loop ($k_{obs} = 0.70 \times 10^{-1}$ min^{-1}) (Fig. 1A) [15]. High activity of the leadzyme with an asymmetric internal loop with five nucleotides was confirmed by structural analysis of mammalian 5S rRNA [16]. The designed leadzyme showed Pb^{2+}-binding capacity and hydrolytic properties (Fig. 2). A 10-fold excess of Pb^{2+} over RNA (leadzyme catalytic strand) was used. A main 37-nucleotide cleavage product was observed. We also observed some nonspecific degradation products, which are probably due to the chemical lability of Py–Pu phosphodiester bonds and the lack of higher-order structure in short RNAs [37,38].

In the leadzyme activity assays *in vivo*, we delivered a short RNA (catalytic RNA) together with metal ions directly to one half of the tobacco leaf. We assume that inhibition of TMV growth in leaves was due to

specific cleavage of TMV RNA (at positions 426 and 427 of TMV RNA). This was manifested by the decreased number of local lesions on infected tobacco leaves treated with catalytic RNA and Pb^{2+}. We found 15–35 local lesions in examined assays vs. 80–110 in controls. Reliable proof of TMV RNA hydrolysis came from the RT-PCR experiments. A high rate of infection observed in reference plants treated with only RNA or Pb^{2+} indicates that neither RNA nor Pb^{2+} alone can account for TMV RNA hydrolysis. The control experiments with tobacco leaves dosed with catalytic RNA and TMV showed high rates of infection (on both the phenotypic and molecular levels), and demonstrated that the exogenous RNA used in this study performs its catalytic function only in the presence of Pb^{2+}. Therefore, the catalytic RNA alone can serve as a noncatalytic negative control. The optimal activity of the leadzyme *in vivo* was observed during $TMV/Pb^{2+}/RNA$ coinoculation and with a two-fold Pb^{2+} excess over the catalytic RNA. This conclusion is consistent with crystallographic data on the leadzyme structure obtained at 1.8 Å. The crystal structure shows two Pb^{2+} bound to the catalytic core. One of the ions participates in structural changes around the cleavage site, and the other binds near the scissile bond [14].

Both macroscopic observation of tobacco leaves and molecular analysis confirmed the effectiveness of exogenously applied ssRNA for specific inhibition of viral expression. Based on the rate of necrotic symptoms, we estimated that around 70% of TMV spreading was stopped (Figs 3B and 4B), so the hydrolytic properties of short ssRNA could be used in antiviral applications. It is surprising that Pb^{2+} can be used as a leadzyme activator. The toxic effects of lead have been linked to many human disorders. The normal blood levels of lead in humans range from 0.1 to 0.2 μM, whereas high levels within the range 0.5–5 μM are known to have deleterious effects on the nervous, renal and reproductive systems [39,40]. There are many aspects of the effect of lead toxicity on a cell level: protein binding [41,42], nonspecific RNA hydrolysis at high concentrations [43,44], and specific RNA hydrolysis due to leadzyme motif formation in *cis* in cellular RNAs [39]. The toxic effects of lead depend on its dose. In our studies, the optimal activity of the leadzyme *in vivo* in *Nicotiana tabacum* plants was observed at 5 μM Pb^{2+}. No other symptoms except necrosis caused by TMV with both 5 μM Pb^{2+} and 10 μM Pb^{2+} were seen in tobacco leaves *in vivo*. Moreover, it was shown that low concentrations of 'stressors' such as Pb^{2+} or other heavy metals can have stimulating effects on the growth [43], photosynthetic oxygen evolution [46,47] and metabolic activity [48] of plants.

In summary, our antiviral strategy based on ssRNA application seems to be very effective. It has the advantages of both interference RNA technology and catalytic nucleic acid application. This short 16-nucleotide, ssRNA is stable in the cell, specifically recognizes target sequences, and hydrolyzes the substrate.

Experimental procedures

Plants and virus

Nicotiana tabacum cv. Xanti-nc plants were used as a local lesion host. The plants were kept in a growth chamber at temperatures within the range 20–25 °C. Five-week-old tobacco leaves were inoculated.

TMV strain U1 was purified from infected *Nicotiana tabacum* cv. 'samsun' by extraction in distilled water or 0.1 M citric buffer, and clarified with chloroform followed by precipitation with polyethylene glycol (PEG-6000) and low-speed (10 000 *g* for 20 min, J2-M1 Beckman, rotor type JA10) and high-speed (75 000 *g* for 2 h, LE-80 Beckman, rotor type 45 TI) centrifugation. The virions were further purified by centrifugation (80 000 *g* for 2 h, LE 80 Beckman, rotor type SW48) in a 10–40% sucrose density gradient. The virus band was collected and concentrated by high-speed centrifugation (75 000 *g* for 2 h, LE-80 Beckman, rotor type 45 TI) and resuspended in water. The concentration of the purified virus was determined spectrophotometrically at 260 nm (BioPhotometer, Eppendorf, Hamburg, Germany).

Purified virus was stored at 4 °C in water [21].

Virus inoculation

Inoculations were carried out on one half of fully expanded leaves of at least three tobacco plants for one assay by gently rubbing the leaf surface with the inoculum. Carborundum was used as an abrasive [22]. The other half of each leaf served as an uninoculated control.

The inoculum used throughout experiments contained: TMV suspension at 5 μg·mL^{-1}, 16-nucleotide-long RNA (catalytic strand of a leadzyme; chemically synthesized in IBA, Berlin, Germany) at concentrations of 2.5–25 μM, AND Pb^{2+} at concentrations of 0.5–10 μM. RNA and Pb^{2+} were mixed together with virus just before inoculation or added separately after 2 and 4 h. In the case of sequential inoculation of RNA and/or Pb^{2+} after previous virus inoculation, the leaves were rinsed with water after TMV inoculation (up to 5 min after infection), and then carborundum was sprayed again just before RNA and/or Pb^{2+} were applied.

After infection, the inoculated plants were kept in a growth chamber initially at 20 °C (first day), and then at 25 °C with a 12 h light and 12 h dark cycle. For the observation of local lesions, inoculated leaves were harvested

and photographed 5 days postinoculation. Finally, the number of necrotic lesions was estimated.

RNA isolation and RT-PCR analysis

Total RNA was extracted from approximately 150 mg of infected leaf tissue using the RNAqueus-Small Scale Phenol-free Total RNA Isolation Kit (Ambion, Austin, TX, USA). Reverse transcription was accomplished using 2 μg of RNA samples, hexamer random primers and the Revert-Aid H Minus First Strand cDNA Synthesis Kit (Fermentas, Vilnius, Lithuania). An aliquot of cDNA was used for PCR amplification with *Taq* polymerase (Fermentas) and TMV-specific primers binding upstream (TMV1: 5'-GCCCAAGGTGAACTTTTCAA-3') and downstream (TMV2: 5'-TAGCGCAATGGCATACACTC-3') of the hydrolysis position as well as β-actin primers (Ambion). PCR was performed with the following conditions: 1 cycle of 94 °C for 2 min, 20 cycles of 94 °C for 30 s, 55 °C for 30 s and 72 °C for 30 s, followed by extension at 72 °C for 5 min. To amplify β-actin cDNA, PCR was carried out with the same conditions, except that the number of cycles was increased to 35. Equal volumes of amplified products were electrophoresed on 1.5% agarose gel, stained with ethidium bromide [23], and quantified by phosphoimager analysis (IMAGEQUANT, version 5.1, Molecular Dynamics, Sunnyvale, CA, USA).

TMV hydrolysis with leadzyme *in vitro*

A 100-nucleotide TMV RNA fragment including the cleavage site of the leadzyme was synthesized by *in vitro* transcription. cDNA TMV was used as a template to amplify 100-bp cDNA TMV with primers TMV3 (upstream) 5'-TAATACGACTCACTATAGGGCGAATAGGCGGGAATTTTGCATC-3' containing the T7 polymerase promoter sequence, and TMV4 (downstream) 5'-CAATACTGTCTTTCTGGCCTTC-3'. TMV RNA was transcribed *in vitro* using the MEGAshortscript T7 High Yield Transcription Kit (Ambion). A 100-nucleotide TMV RNA fragment was purified, labeled at the 5'-end with $[\gamma\text{-}^{32}P]ATP$ and 10 U of T4 polynucleotide kinase (Epicentre, Madison, WI, USA) and separated by 10% PAGE with 7 M urea. The radioactive band was cut off, and RNA was eluted with water and precipitated with ethanol.

The leadzyme cleavage reaction of TMV RNA was performed in 15 mM Mops (pH 7.5) buffer at 25 °C. Thirty thousand counts per minute of the labeled and 250 nM unlabeled RNA substrate was mixed with 25 μM RNA leadzyme catalytic strand, heated up to 90 °C for 2 min, cooled slowly (1 °C·min^{-1}) to 25 °C, and incubated at 25 °C for 60 min. The reaction was initiated by addition of Pb^{2+} just before incubation and stopped by addition of an equal volume of loading buffer (25 mM sodium citrate, pH 5.1, 1 mM EDTA, 7 M urea, 0.1% xylene cyanol, 0.1%

bromophenol blue). The reaction products were analyzed by 10% PAGE with 7 M urea (pH 8.3). The hydrolysis site was estimated using an RNA marker (29 nucleotides) and an alkaline RNA ladder, in 50 mM NaOH and 1 mM EDTA for 90 s at 95 °C [16].

Bioinformatic analysis

The genomic sequences of TMV RNA was obtained from the National Center for Biotechnology Information Gene-Bank database [24]. The RNA secondary structures of the TMV target sequences were predicted using the MFOLD program (http://www.bioinfo.rpi.edu/applications/mfold) [25]. Primers for PCR reactions were designed using the PRIMER3 program (http://frodo.wi.mit.edu/cgi-bin/primer3/primer3_www.cgi) [26]. Statistical analysis was performed using Microsoft Excel and IMAGEQUANT.

Acknowledgements

References

1 Peracchi A (2004) Prospects for antiviral ribozymes and deoxyribozymes. *Rev Med Virol* **14**, 47–64.

2 Schubert S & Kurreck J (2004) Ribozyme- and deoxyribozyme-strategies for medical applications. *Curr Drug Targets* **5**, 667–681.

3 Sullenger BA & Gilboa E (2002) Emerging clinical application of RNA. *Nature* **418**, 252–258.

4 Burke DH & Greathouse ST (2005) Low-magnesium, *trans*-cleavage activity by type III, tertiary stabilized hammerhead ribozymes with stem I discontinuities. *BMC Biochem* **6**, 14–25.

5 Li Y & Breaker R (1999) Kinetics of RNA degradation by specific base catalysis of transesterification involving the 2'-hydroxyl group. *J Am Chem Soc* **121**, 5364–5372.

6 Beigelman L, McSwiggen JA, Draper KG, Gonzalez C, Jensen K, Karpeisky AM, Modak AS, Matulic-Adamic J, DiRenzo AB, Haeberli P *et al.* (1995) Chemical modification of hammerhead ribozymes. Catalytic activity and nuclease resistance. *J Biol Chem* **270**, 25702–25708.

7 Burlina F, Favre A & Fourrey JL (1997) Chemical engineering of RNase resistant and catalytically active hammerhead ribozymes. *Bioorg Med Chem* **5**, 1999–2010.

8 Usman N & Blatt LM (2000) Nuclease-resistant synthetic ribozymes: developing a new class of therapeutics. *J Clin Invest* **106**, 1197–1202.

9 Pan T & Uhlenbeck OC (1992) A small metalloribozyme with a two-step mechanism. *Nature* **358**, 560–563.

10 Pan T & Uhlenbeck OC (1992) *In vitro* selection of RNAs that undergo autolytic cleavage with Pb^{2+}. *Biochemistry* **31**, 3387–3895.

11 Legault P, Hoogstraten CG, Metlitzky E & Pardi A (1998) Order, dynamics and metal-binding in the lead-dependent ribozyme. *J Mol Biol* **248**, 325–335.

12 Hoogstraten CG, Wank JR & Pardi A (2000) Active site dynamics in the lead-dependent ribozyme. *Biochemistry* **39**, 9951–9958.

13 Wedekind JE & McKay DB (1999) Crystal structure of lead-dependent ribozyme revealing metal binding sites relevant to catalysis. *Nat Struct Biol* **6**, 261–268.

14 Wedekind JE & McKay DB (2003) Crystal structure of the leadzyme at 1.8 Å resolution: metal ion binding and the implications for catalytic mechanism and allo site ion regulation. *Biochemistry* **42**, 9554–9563.

15 Ohmichi T, Okumoto Y & Sugimoto N (1998) Effect of substrate RNA sequence on the cleavage reaction by a short ribozyme. *Nucleic Acids Res* **26**, 5655–5661.

16 Barciszewska MZ, Wyszko E, Bald R, Erdman VA & Barciszewski J (2003) 5S rRNA is a leadzyme. A molecular basis for lead toxicity. *J Biochem* **133**, 309–315.

17 Kuiken T, Fouchier R, Rimmelzwaan G & Osterhaus A (2003) Emerging viral infections in a rapidly changing world. *Curr Opin Biotechnol* **14**, 641–646.

18 Cockerill FR 3rd & Smith TF (2004) Response of the clinical microbiology laboratory to emerging (new) and reemerging infectious diseases. *J Clin Microbiol* **42**, 2359–2365.

19 Fauci AS, Touchette NA & Folkers GK (2005) Emerging infectious diseases: a 10-year perspective from the National Institute of Allergy and Infectious Diseases. *Emerg Infect Dis* **11**, 519–525.

20 Soosaar JL, Burch-Smith TM & Dinesh-Kumar SP (2005) Mechanism of plant resistance to viruses. *Nat Rev Microbiol* **3**, 789–797.

21 Pospieszny H, Borodynko N & Jonczyk M (2003) First report of tobacco mosaic (TMV) in natural infection of black locust (*Robinia pseudoacacia*) in Poland. *Phytopathol Pol* **30**, 27–35.

22 Matthews REF (1991) *Plant Virology*, 3rd edn. Academic Press, San Diego, CA.

23 Ausubel FM, Brnet R, Kingston RE, Moore DD, Seidman JG, Smith JA & Struhl K, eds. (1992) *Short Protocols in Molecular Biology*, 2nd edn. *A Compendium of Methods from Current Protocols in Molecular Biology*. Greene Publishing Associates and John Wiley & Sons, New York.

24 http://www.ncbi.nlm.nih.gov/Genbank/.

25 Zuker M, Mathews DH & Turner DH (1999) Algorithms and thermodynamics for RNA secondary structure prediction: a practical guide. In *RNA Biochemistry and Biotechnology* (Barciszewski J & Clark BFC, eds), pp. 11–43. NATO ASI Series. Kluwer, Academic Publishers, Dordrecht.

26 Rozen S & Skaletsky H (2000) Primer3 on the WWW for general users and for biologist programmers. *Methods Mol Biol* **132**, 365–386.

27 Citti L & Rainaldi G (2005) Synthetic hammerhead ribozymes as a therapeutic tools to control disease genes. *Curr Gene Ther* **5**, 11–24.

28 Khan AU & Lal SK (2003) Ribozymes: a modern tool in medicine. *J Biomed Sci* **10**, 457–467.

29 Puerta-Fernandez E, Romero-Lopez C, Barroso-del Jesus A & Berzal-Herranz A (2003) Ribozymes: recent advances in the development of RNA tools. *FEMS Microbiol Rev* **27**, 75–97.

30 Hughes MD, Hussain M, Nawaz Q, Sayyed P & Akhtar S (2001) The cellular delivery of antisense oligonucleotides and ribozymes. *Drug Discov Today* **6**, 303–315.

31 Waterhouse PM, Wang M-B & Lough T (2001) Gene silencing as an adaptive defense against viruses. *Nature* **411**, 834–842.

32 Saksela K (2003) Human viruses under attack by small inhibitory RNA. *Trends Microbiol* **8**, 345–347.

33 Hannon GJ (2002) RNA interference. *Nature* **418**, 244–251.

34 Voinnet O (2005) Induction and suppression of RNA silencing: insights from viral infections. *Nat Rev* **6**, 206–220.

35 Jackson AL & Linsley PS (2004) Noise amidst the silence: off-target effects of siRNAs? *Trends Genet* **11**, 521–524.

36 Dillon CP, Sandy P, Nencioni P, Kissler S, Rubinson DA & Van Parijs L (2005) RNAi as an experimental and therapeutic tool to study and regulate physiological and disease processes. *Annu Rev Physiol* **67**, 147–173.

37 Kierzek R (1992) Hydrolysis of oligoribonucleotides: influence of sequence and length. *Nucleic Acids Res* **20**, 5073–5077.

38 Kierzek R (1992) Nonenzymatic hydrolysis of oligoribonucleotides. *Nucleic Acids Res* **20**, 5079–5084.

39 Barciszewka MZ, Szymanski M, Wyszko E, Pas J, Rychlewskim L & Barciszewski J (2005) Lead toxicity through the leadzyme. *Mut Res* **589**, 103–110.

40 Patocka J & Cerny K (2003) Inorganic lead toxicology. *Acta Med (Hradec Karlowe)* **46**, 65–72.

41 Hanas JS, Rodgers JS, Bantle JA & Cheng YG (1999) Lead inhibition of DNA-binding mechanism of Cys_2Hys_2 zinc finger proteins. *Mol Pharmacol* **56**, 982–988.

42 Payne JC, ter Horst MA & Godwin HA (1999) Lead fingers: Pb^{2+} binding to structural zinc-binding domains determined directly by monitoring lead-thiolate charge-transfer bands. *J Am Chem Soc* **121**, 6850–6855.

43 Dirheimer G, Ebel JP, Bonnet J, Gangloff J, Keith G, Krebs B, Kuntzel B, Roy A, Weissenbach J & Werner

C (1972) Primary structure of transfer RNA. *Biochimie* **54**, 127–144.

44 Werner C, Krebs B, Keith G & Dirheimer G (1976) Specific cleavages of pure tRNAs by plumbous ions. *Biochim Biophys Acta* **432**, 161–175.

45 Ernst WHO, Verkleij JAC & Schat H (1992) Metal tolerance in plants. *Acta Bot Neerl* **41**, 229–248.

46 Nyitrai P, Boka K, Gaspar L, Sarvari E, Lenti K & Keresztes A (2003) Characterization of the stimulating effect of low-dose stressors in maize and bean seedlings. *J Plant Physiol* **160**, 1175–1183.

47 Nyitrai P, Boka K, Gaspar L, Sarvari E & Keresztes A (2004) Rejuvenation of aging bean leaves under the effect of low-dose stressors. *Plant Biol* **6**, 708–714.

48 Prasad MNV, Malec P, Waloszek A, Bojko M & Strzaka K (2001) Physiological responses of *Lemna triscula* L. (duckweed) to cadmium and copper bioaccumulation. *Plant Sci* **161**, 881–889.

49 Brigneti GO, Voinnet O, Li WX, Ji LH, Ding SH & Baulcombe DC (1998) Viral pathogenicity determinants are suppressors of transgene silencing in *Nicotiana benthamiana*. *EMBO J* **17**, 6739–6746.

50 Kasschau KD, Xie Z, Allen E, Llave C, Chapman EJ, Krizan KA & Carrington JC (2003) P1/HC-Pro, a viral suppressor of RNA silencing, interferes with *Arabidopsis* development and miRNA function. *Dev Cell* **4**, 205–217.

51 Voinnet O, Lederer C & Baulcombe DC (2000) A viral movement protein prevents spread of the gene silencing signal in *Nicotiana benthamiana*. *Cell* **103**, 157–167.

52 Kubota K, Tsuda S, Tamai A & Meshi T (2003) Tomato mosaic virus replication protein suppresses virus-targeted posttranscriptional gene silencing. *J Virol* **77**, 11016–11026.